

MULTICARRIER WAVE DUAL REFERENCE VERY LOW FREQUENCY PWM CONTROL OF A NINE LEVELS NPC MULTI-STRING THREE PHASE INVERTER TOPOLOGY FOR PHOTOVOLTAIC SYSTEM CONNECTED TO THE MEDIUM ELECTRIC GRID

¹RABIAA.Mechouma, ²HANIA.Aboub, ³BOUBAKEUR.Azoui

^{1,2,3}LEB University de Batna, Algérie, ¹rabiaa.mechouma@yahoo.com, ²haniaaboub@gmail.com, ³azoui_b@yahoo.com

Abstract: *The multilevel multi-string inverter has gained much attention in recent years due to its advantages in lower switching loss, better electromagnetic compatibility, higher voltage capability, and lower harmonics. Solar Energy is one of the favorable renewable energy resources and the multilevel inverter has been proven to be one of the important enabling technologies in photovoltaic (PV) utilization. This paper proposes a diode-clamped three phase nine levels grid connected photovoltaic inverter topology with a multicarrier dual reference pulse-width modulated (PWM) control scheme. Eight carrier waves of the same frequency and different amplitudes are compared with two references (a sine wave and its opposite) for generating the control signals of the switches. Some DC/DC boost converters are used to amplify the voltage produced by the photovoltaic generators. Each of these converters is controlled by an MPPT algorithm in order to track the maximum power point of the GPV; Results of simulation in Matlab environment are given and discussed.*

Keywords: *Grid connected photovoltaic (PV) system, diode-clamped multilevel three phase multi-string inverter, multicarrier PWM, and medium voltage grid.*

1. Introduction

A multilevel inverter is a power electronic device built to synthesize a desired AC voltage from several levels of DC voltages. Such inverters have been the subject of research in the last several years where the DC levels were considered to be identical in that all of them were capacitors, batteries, solar cells, etc. [1]. It has gained much attention due to its advantages in lower switching loss, better electromagnetic compatibility, higher voltage capability, and lower harmonics. Multilevel inverters, including an array of power semiconductors and capacitor voltage sources, the output of which generate voltages with stepped waveforms. The commutation of the switches permits the addition of the capacitor voltages, which reach high

voltage at the output, while the power semiconductors must withstand only reduced voltages. Photovoltaic (PV), wind energy and hydro conversion are the most explored technologies due to their considerable advantages [2-3], such as reliability, reasonable installation and energy production costs, low environmental impact, capability to support micro grid systems and to connect to the electric grid [4]. A schematic diagram of one phase leg of inverters with different numbers of levels is shown, in Fig.1 for which the action of the power semiconductors is represented by an ideal switch with several positions. In this paper, we present a multi carrier dual reference very low frequency diode-clamped three phase 09 level inverter designed for photovoltaic system connected to a medium voltage grid. This inverter is controlled by a PWM strategy based on the comparison of several carrier waves with two reference signals. More control signals are obtained. Instead of a single photovoltaic generator at the input of the inverter, we have a multiple continuous source which is composed of several photovoltaic generators. Each of them consists of N_P branches, each of which is composed of N_S solar panels in series. Each generator of this source generates a voltage which is amplified at the output by means of a dc / dc converter. This converter is controlled by an MPPT algorithm. The overall system is shown in Fig.2. The study is simulated in Matlab/Simulink and results are given and discussed.

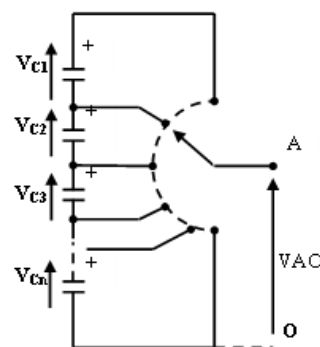


Fig.1 One phase leg of an inverter with “n” levels

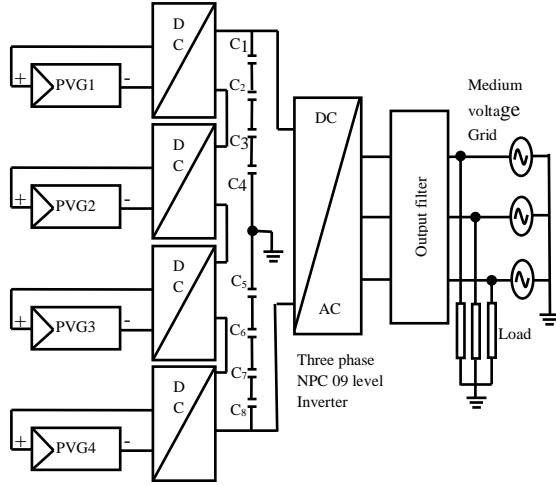


Fig. 2 Schematic diagram of the overall PV system

2. Modeling of the global grid connected photovoltaic system structure

Modeling photovoltaic system is required as a crucial step to describe the functioning of all the elements that are all starting from the DC source arriving to the grid. It predicts the conceptual and energy performance of PV systems connected to the grid in different climatic conditions and under well-defined loads. Models of the various components will be presented as follows:

2.1 Model of the photovoltaic source

As already mentioned, the photovoltaic source consists of 04 parts, each of them represents a partial photovoltaic generator. Each partial PVG generates at its output a DC voltage which is then amplified by a DC / DC converter. Continuous output voltages of the converters are then summed to obtain an overall voltage that feeds the inverter. The equivalent circuit diagram of a PV cell is illustrated in fig.3

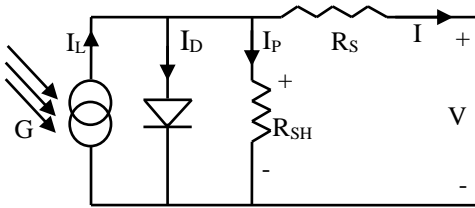


Fig.3 Equivalent circuit diagram of a PV cell

The selected model in this work is inspired from references [5-7]. The advantage of this model can be established using only standard data for the module and cells provided by the manufacturer in the technical data (data and graphs). It is independent of the saturation current I_s of the diode (see Fig. 3). The current supplied by the solar module (I_M) in any conditions, is given by:

$$I_M = I_{SCM} \left[1 - \left\{ \exp \left(\frac{V_M - V_{OCM} + I_M R_{SM}}{n V_{THM}} \right) - \exp \left(\frac{-V_{OCM}}{n V_{THM}} \right) \right\} \right] \quad (1)$$

Where:

I_{SCM} and V_{OCM} are respectively the short circuit current and the open circuit voltage at the standard test conditions (STC), I_M and V_M are respectively the current and the voltage delivered by the module at any conditions, R_{SM} is the series resistance of the module, V_{THM} is the thermal voltage and n is the quality factor which varies typically from 1 to 2.

V_{OCM} and I_{SCM} are given by:

$$V_{OCM} = V_{OCC} \times N_{SC} \quad (2)$$

$$I_{SCM} = I_{SCC} \times N_{PC} \quad (3)$$

The thermal voltage is given by:

$$V_{THM} = V_{THC} \times N_{SC} \quad (4)$$

$$\text{Where: } V_{THC} = \frac{k T_C}{q}$$

The series resistance of the module is given by:

$$R_{SM} = \frac{N_{SC}}{N_{PC}} R_{SC} \quad (5)$$

Where:

V_{THC} is the thermal voltage of the PV cell, R_{SC} is the series resistance of the PV cell, k is the Boltzmann's constant, q is the electrical charge of the electron, N_{PC} is the number of branches of parallel cells in a module and N_{SC} is the series number of cells of each branch.

The open circuit voltage of the PV cell is given by:

$$V_{OCC} = V_{OCC-ref} - \beta(T - T_{ref}) \quad (6)$$

Where: $V_{OCC-ref}$ is the open circuit voltage of the PV cell in standard conditions, T_{ref} is the reference value of the temperature ($T_{ref}=25^\circ\text{C}$) and T is the operating temperature of the PV cell, it is given by:

$$T = T_a - T_{ref} \quad (7)$$

T_a is ambient temperature of the PV cell.

The thermal voltage of the PV cell can be easily calculated using the coordinates of the maximum power point of the cell (V_{MPPC} and I_{MPPC}). The expression of V_{THC} is:

$$V_{THC} = \frac{V_{MPPC} + R_{SC} I_{MPPC} - V_{OCC}}{\ln \left(1 - \frac{I_{MPPC}}{I_{SCC}} \right)} \quad (8)$$

The current delivered by each PVG is given by the following expression:

$$I = N_P I_{SCM} \left[1 - \left\{ \exp \left(\frac{N_S V_M - N_S V_{OCM} + N_P I_{SM} R}{n N_S V_{THM}} \right) - \exp \left(\frac{-V_{OCM}}{n V_{THM}} \right) \right\} \right] \quad (9)$$

2.2 DC/DC Boost converter and its control

2.2.1 DC/DC Boost converter model

A boost converter (step-up converter) is a DC-to-DC power converter with an output voltage greater than its input voltage. A schematic of a boost power stage is shown in Fig.4. The basic principle of a Boost converter consists of two distinct states.

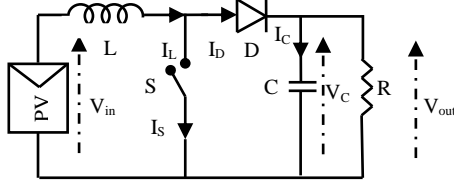


Fig. 4 DC/DC Boost converter schematic

a) In the On-state, the switch “S” is closed, resulting in an increase of the inductor current I_L , V_{in} is given as follows:

$$V_{in} = L \frac{dI_L}{dt} \quad (10)$$

If $x_1 = I_L$ and $x_2 = V_C$ the state equations are given by:

$$\begin{cases} \dot{x}_1 = \frac{V_{in}}{L} \\ \dot{x}_2 = \frac{1}{C} I_C = \frac{1}{RC} V_{out} \end{cases} \quad (11)$$

$$V_{out} = V_C = x_2 \quad (12)$$

In matrix form the system of equations (11) and (12) becomes:

$$\begin{bmatrix} \dot{x}_1 \\ \dot{x}_2 \end{bmatrix} = \begin{bmatrix} 0 & 0 \\ 0 & \frac{1}{RC} \end{bmatrix} \begin{bmatrix} x_1 \\ x_2 \end{bmatrix} + \begin{bmatrix} \frac{1}{L} \\ 0 \end{bmatrix} V_{in} \quad (13)$$

$$V_{out} = C_1 \begin{bmatrix} x_1 \\ x_2 \end{bmatrix} \quad (14)$$

$$\text{If: } A_1 = \begin{bmatrix} 0 & 0 \\ 0 & \frac{1}{RC} \end{bmatrix}, B_1 = \begin{bmatrix} \frac{1}{L} \\ 0 \end{bmatrix}, C_1 = [0 \quad 1]$$

We obtain:

$$\begin{bmatrix} \dot{x}_1 \\ \dot{x}_2 \end{bmatrix} = A_1 \begin{bmatrix} x_1 \\ x_2 \end{bmatrix} + B_1 V_{in} \quad (15)$$

b) In the Off-state, the switch “S” is open and the only path offered to inductor current is through the flyback diode D, the capacitor C and the load R. Differential equations that govern the operation of the circuit are:

$$L \frac{dI_L}{dt} = V_{in} - V_C \quad (16)$$

$$C \frac{dV_C}{dt} = I_L - I_{out} \quad (17)$$

By substituting I_L by the state variable x_1 , and V_C by the state variable x_2 , the above equations become:

$$\begin{cases} \dot{x}_1 = \frac{1}{L} V_{in} - \frac{1}{L} x_2 \\ \dot{x}_2 = \frac{1}{C} x_1 - \frac{1}{RC} x_2 \end{cases} \quad (18)$$

In matrix form the system of equations (18) becomes:

$$\begin{bmatrix} \dot{x}_1 \\ \dot{x}_2 \end{bmatrix} = \begin{bmatrix} 0 & -\frac{1}{L} \\ \frac{1}{C} & -\frac{1}{RC} \end{bmatrix} \begin{bmatrix} x_1 \\ x_2 \end{bmatrix} + \begin{bmatrix} \frac{1}{L} \\ 0 \end{bmatrix} V_{in} \quad (19)$$

If:

$$A_2 = \begin{bmatrix} 0 & -\frac{1}{L} \\ \frac{1}{C} & -\frac{1}{RC} \end{bmatrix}, B_2 = \begin{bmatrix} \frac{1}{L} \\ 0 \end{bmatrix}, C_2 = [0 \quad 1]$$

Then:

$$\begin{bmatrix} \dot{x}_1 \\ \dot{x}_2 \end{bmatrix} = A_2 \begin{bmatrix} x_1 \\ x_2 \end{bmatrix} + B_2 V_{in} \quad (20)$$

Finally, for a full period of operation (T) and by adding the two equations (15) and (20) the system of equations becomes:

$$\begin{bmatrix} \dot{x}_1 \\ \dot{x}_2 \end{bmatrix} = \left(A_1 \begin{bmatrix} x_1 \\ x_2 \end{bmatrix} + B_1 V_{in} \right) D + \left(A_2 \begin{bmatrix} x_1 \\ x_2 \end{bmatrix} + B_2 V_{in} \right) (1-D) \quad (21)$$

After rearranging equation (21), the matrix form is:

$$\begin{bmatrix} \dot{x}_1 \\ \dot{x}_2 \end{bmatrix} = (A_1 D + A_2 (1-D)) \begin{bmatrix} x_1 \\ x_2 \end{bmatrix} + (B_1 D + B_2 (1-D)) V_{in} \quad (22)$$

Where:

$A = (A_1 D + A_2 (1-D))$, $B = B_1 D + B_2 (1-D)$ are respectively the state matrix and the control matrix. D is the duty cycle, it represents the fraction of the commutation period T during which the switch “S” is on. Therefore D ranges between 0 (“S” is never on) and 1 (“S” is always on).

2.2.2 MPPT Control

The boost (step-up) DC / DC converter is modeled as a block whose inputs are the voltage delivered by the solar panels and the second input is the duty cycle D generated by the Maximum Power Point Tracking (MPPT) controller. This MPPT is used on the basis of a search algorithm called perturb and observe (P & O) [8].

2.3 Model of the three-Phase nine levels NPC Inverter

Fig. 5 shows the diagram of the three-Phase nine levels Neutral Point Clamped (NPC) inverter.

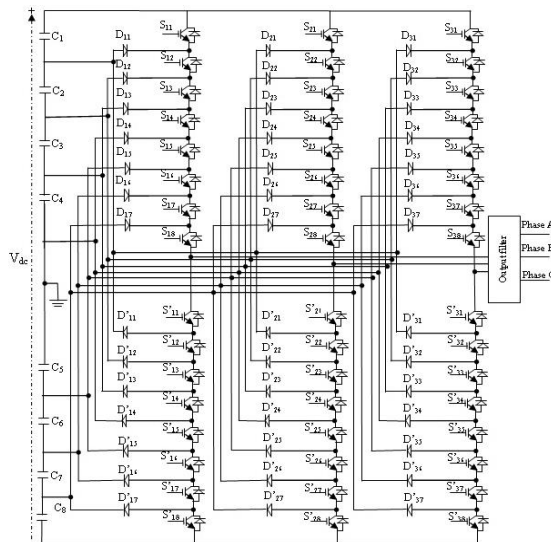


Fig.5 Diagram of the diode-clamped three-phase nine levels inverter

It is composed of three arms; each one of them is composed of sixteen IGBTs that are noted as “ S_{ij} ”. The index (i) indicates the phase: if $i = 1$, it means the phase “A”, $i=2$ the phase “B” and $i=3$ the phase “C”. The index (j) indicates the number of the switches noted as: $S_{11}, S_{12}, S_{13}, S_{14}, S_{15}, S_{16}, S_{17}$ and S_{18} form the upper part of the arm in each phase and the switches noted as: $S'_{11}, S'_{12}, S'_{13}, S'_{14}, S'_{15}, S'_{16}, S'_{17}$ and S'_{18} form the lower part of the arm in each phase. Each arm of the inverter also comprises fourteen clamped diodes, which are denoted “ D_{ij} ”. The output of the inverter is connected to the electric grid through a filter. The diode-clamped inverter can generate 09 voltage levels: four levels are positive, one level is zero and four levels are negative. The inverter is composed of 48 switches, hence the necessity de 48 control signals. These signals can be generated by a PWM controller.

2.4 Control circuit of the inverter

The control circuit of the inverter is shown in Fig.6. It is based on the use of the PWM strategy in a closed loop current. This strategy consists in comparing eight carrier signals of the same frequency ($f_c=400\text{Hz}$) with a sinusoidal

reference signal. PI controllers are also used; they are characterized by their coefficients K_i and K_p ($K_i=0.01$; $K_p=0.01$). A square signal is added. As has already been mentioned, each arm of the inverter is composed of sixteen IGBTs, hence the necessity of sixteen control signals. So for these control signals, a small Matlab program is performed.

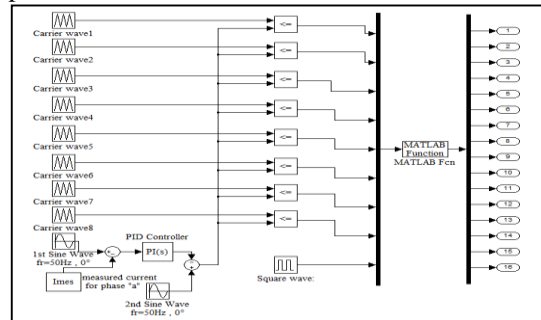


Fig.6 Control circuit of one arm of the inverter (Phase “a”)

3. Simulation of the overall system

The overall diagram of the simulation is shown in Fig. 7.

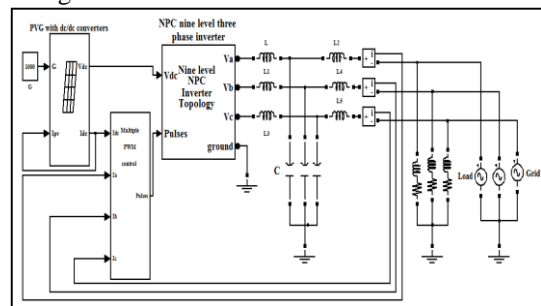


Fig.7 Simulation scheme of the overall system

and the PV source is presented with the DC/DC converters in Fig.8.

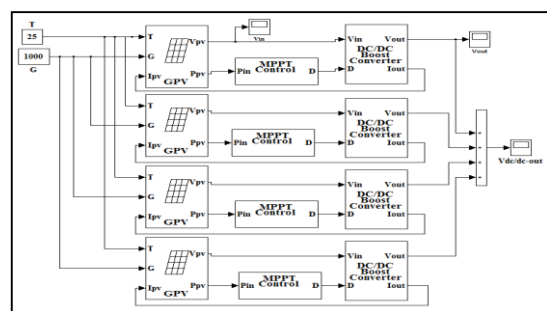


Fig.8 Overall structure of the PV source with DC/DC converters

The simulation results are:

3.1 Characteristic of the PV source

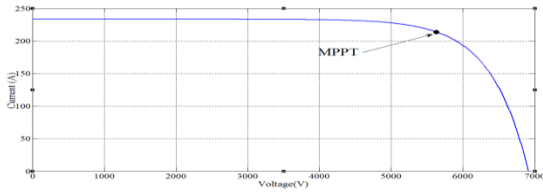


Fig. 9 Characteristic of the photovoltaic source under STC ($G=1000W/m^2$ and $T=25^\circ C$)

3.2 Parameters of the DC/DC converters

Fig. 10 illustrates the voltage at the input and the output of the DC/DC converter.

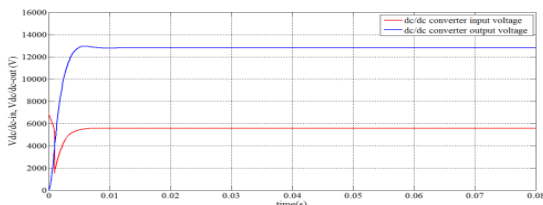


Fig.10 DC/DC converters input and output voltage

The amplification voltage is very clear. The voltage value of 5536V, generated by the PV source, becomes 12660V at the output of DC/DC converters in series.

3.3 Parameters of the NPC inverter

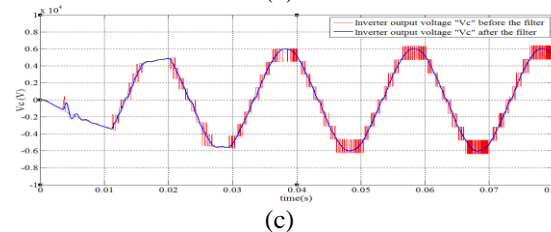
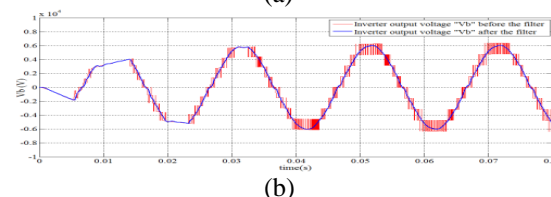
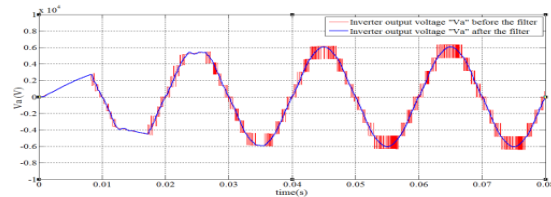


Fig.11 Inverter output voltage before and after the filter: (a) Phase "a", (b) Phase "b", (c) Phase "c"

Fig. 11 shows the voltages at the inverter output before and after the filter. For each phase, the voltage before filtering, has a shape of a staircase waveform, with a maximum value of $6330V=V_{dc}/2$. However, the voltage after filtering is sine wave that begins with a transitional phase during a time of 0.03s.

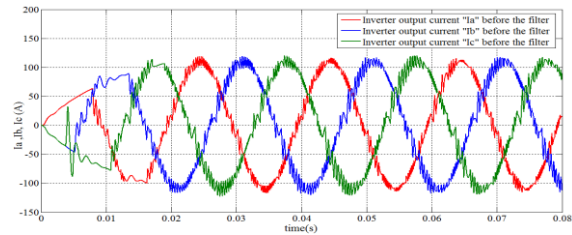


Fig.12 Inverter output currents before the filter

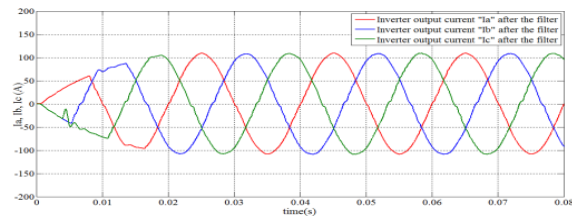


Fig.13 Inverter output currents after the filter (with grid disconnected)

The currents, obtained after filtering, at the output of the inverter are shown in Figures 12 and 13. Their shapes are sinusoidal with a substantially maximum value of 110A. When the grid is connected the current wave forms are presented as follows:

Figs 15, 16 and 17 show the output current of the inverter for three phases "a", "b" and "c". It is obvious that in a radiation intensity ($G=1000W/m^2$) which is a high intensity, the output current after the filter is the sum of the current in the load and that injected in the grid.

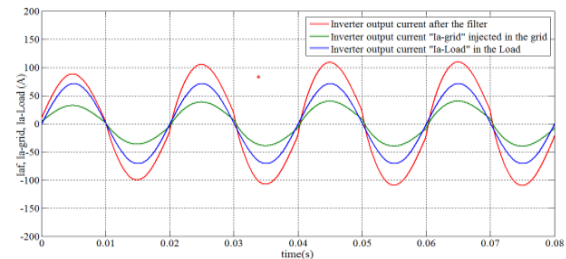


Fig. 14 Inverter output current for phase "a" (a) current after the filter , (b) current injected in the grid , (c) current in the load(blue)

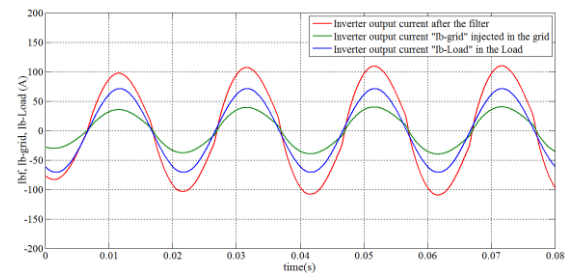


Fig. 15 Inverter output current for phase "b" current after the filter(red), current injected in the grid (green), current in the load(blue)

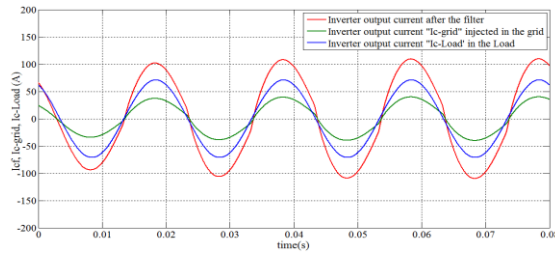


Fig. 16 Inverter output current for phase “c” current after the filter(red), current injected in the grid (green), current in the load(blue)

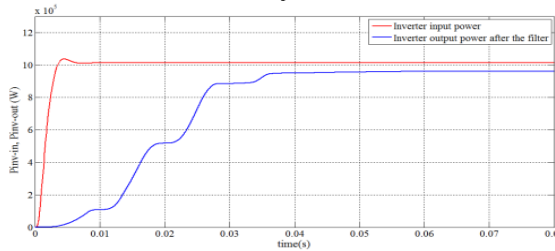


Fig.17 DC/DC converter and Inverter output power

As illustrated in Fig. 18, the inverter input power is 1.05MW, however, the power at its output (after the filter) is 0.98MW, giving an efficiency of 94%.

4. Conclusion

In this paper, a multicarrier wave dual reference very low frequency PWM control of a diode-clamped nine levels multi-string three phase inverter topology for photovoltaic system connected to the medium electric grid has been presented. This control was based on the PWM strategy which used eight carrier signals with different amplitudes, and with the same frequency (equal to 400Hz) which is a very low value. The results are quite interesting. The efficiency of the inverter is very satisfying. However, the disadvantages of this system are the presence of a filter at the output, causing losses by Joule effect and the use of multiple carrier signals for the control of the inverter. So to remedy this, it is preferable to use an inverter that output has more than nine levels in order to avoid the filter, and reduce the number of carrier signals in the control of the inverter. On the other hand, the PV system requires a large number of solar modules with a power of 75W which requires a large area to install, so it is preferable to replace them by more powerful solar modules.

5. References

[1] Vijay Kumar M.G, Manjunath D and Anil W. Patil.:*Comparison of multilevel inverters with PWM Control Method*. International Journal of IT, Engineering and Applied Sciences Research (IJIEASR), ISSN: 2319-4413, Vol.1, N°3, December 2012.

[2] F. Kininger.: *Photovoltaic systems technology*. Kassel, Germany: Universität Kassel, Institut für Available at: www.uni-kassel.de/re.

[3] *Key world energy statistics - 2009*, International Energy Agency (IEA), 2009. Available at: <http://www.iea.org>.

[4] *Global Market Outlook for Photovoltaics Until 2014*, European Photovoltaic Industry Association (EPIA). Available at: <http://www.epia.org>.

[5] A. D. Hansen et al.: *Models for Stand.Alone PV Systems*. Report Riso-R-1219(EN) SEC, RNL, Roskilde, Denmark, 2000.

[6] L. Castaner et S. Silvester. : *Modeling Photovoltaic Systems Using PSPICE*. Wily, 1^{ère} Édition ISBN 0-470-84528-7, 2002.

[7] A. N. Celik et N.Acikgoz. : *Modeling and Experimental Verification of the Operating Currents of Mono-Crystalline Photovoltaic Modules using Four and Five Parameters Models*. Applied Energy, Vol.84, pp. 1-15, Issue 1, January 2007.

[8] J. Surya Kumari, Dr. Ch. Sai Babu, A. Kamalakar Babu. : *Design and Analysis of P&O and IP&O MPPT Techniques for Photovoltaic System*. International Journal of Modern Engineering Research (IJMER), (IJMER), Vol.2, Issue.4, pp.2174-2180, July-Aug. 2012.

Annex

Parameters of ENIESOLAR module used in this work:

Parameter	value
Maximal power P_{MPP}	75W, +/- 10%
Short circuit current I_{SC}	4.67A
Open circuit voltage V_{OC}	21.6V
MPP voltage V_{MPP}	17.30V
MPP current I_{MPP}	4.34A
minimum value of the fuse in series	10A
number of cells in series	36
number of cells in parallel	1